

ORIGINAL RESEARCH ARTICLE

Crop Physiology & Metabolism

Kernel weight responses to the photothermal environment in maize dent × flint and flint × flint hybrids

Ignacio R. Hisse^{1,2}  | Karina E. D'Andrea^{1,2}  | María E. Otegui^{1,3} 

¹ Dep. de Producción Vegetal, Facultad de Agronomía, Univ. de Buenos Aires, Av. San Martín 4453 (C1417DSE), Ciudad de Buenos Aires, Argentina

² Consejo Nacional de Investigaciones Científicas y Técnicas (CONICET), Ciudad de Buenos Aires, Argentina

³ Consejo Nacional de Investigaciones Científicas y Técnicas (CONICET) en INTA, Centro Regional Buenos Aires Norte, Estación Experimental Agropecuaria, Ruta 32 km 4.5, Pergamino, Provincia de Buenos Aires C2700, Argentina

Correspondence

Ignacio R. Hisse, Dep. de Producción Vegetal, Facultad de Agronomía, Univ. de Buenos Aires, Av. San Martín 4453 (C1417DSE), Ciudad de Buenos Aires, Argentina.
Email: hisse@agro.uba.ar

Associate Editor Carlos Messina

Abstract

Maize (*Zea mays* L.) grain yield is assumed to be source limited during the flowering period but sink limited during grain growth; however, environmental restrictions during active grain filling may strongly affect final kernel weight (KW). In this study, we evaluated the effect of natural changes in photothermal conditions during *lag* phase (LP) and effective grain-filling period (EGFP) on KW, its physiological determinants, and the post-flowering source–sink relationships of flint and semident germplasm. F₁ hybrids of flint × flint and dent × flint background were tested during four seasons (Y1, Y2, Y3, and Y4). Across years, the highest KW (286 mg) was obtained under the maximum photothermal quotients during LP ($PTQ_{LP} = 1.18 \text{ MJ m}^{-2} \text{ }^{\circ}\text{C}^{-1}$) and EGFP ($PTQ_{EGFP} = 1.07 \text{ MJ m}^{-2} \text{ }^{\circ}\text{C}^{-1}$) of Y2, whereas the smallest KW (252 mg) and source–sink ratio during grain filling was obtained under the lowest PTQ_{EGFP} ($.79 \text{ MJ m}^{-2} \text{ }^{\circ}\text{C}^{-1}$) of Y3. Supra-optimum temperatures during LP of Y3 negatively affected potential KW determination, and hence kernel growth rate ($P < .001$) as a result of reduced assimilate availability per kernel. Hybrids dent × flint exhibited higher grain yield, kernel number, and plant growth around flowering than flint × flint throughout evaluated seasons but had reduced source–sink relationship during grain filling ($P < .05$) and increased KW sensitivity ($P < .001$) to changes in the photothermal conditions. Results emphasized the importance of the photothermal environment during grain filling on KW determination (particularly for seasons with great photothermal imbalance between filling subphases) as well as the dependency of KW responses on the genetic background.

Abbreviations: D × F, dent by flint; EGFP, effective grain-filling period; F × F, flint by flint; GG, genotypic group; IPTQ, photothermal quotient on intercepted solar radiation basis; KGR, kernel growth rate; KMV, maximum kernel volume; KMWC, maximum kernel water content; KNP, kernel number per plant; KW, kernel weight; KWe, estimated kernel weight; KWm, mean kernel weight; LP, *lag* phase; PCA, principal component analysis; PG_{EGFP} , plant growth during the effective grain-filling period; PGR_{CP} , plant growth rate during the critical period for kernel set; PGY, plant grain yield; PTQ, photothermal quotient; PTQ_{EGFP} , PTQ during the effective grain-filling period; PTQ_{LP} , PTQ during the *lag* phase; VPD_{EGFP} , vapor pressure deficit during the effective grain-filling period; VPD_{LP} , vapor pressure deficit during the *lag* phase; Y, year.

1 | INTRODUCTION

Final individual kernel weight (KW) of maize (*Zea mays* L.) is mainly dependent upon assimilates available per kernel (i.e., the source–sink relationship) during the critical period for kernel set (~30 d centered at silking), when potential KW is established (Gambín et al., 2006, 2008). Assimilate availability during the subsequent effective grain-filling period (EGFP) is not expected to restrict kernel growth of most early-sown crops (Borrás et al., 2004), revealing that both grain-filling subphases (i.e., *lag* phase [LP] and EGFP) are dynamically interrelated to each other. However, stressful conditions such as water deficit (Ouattar, Jones, & Crookston, 1987; Ouattar, Jones, Crookston, & Kajeiou, 1987), above-optimum temperatures (Rattalino Edreira et al., 2014), or reduced nitrogen offer (Hisse et al., 2019) during the effective grain filling may reduce the plant capacity to provide assimilates to growing kernels, and consequently limit the achievement of their potential size (Borrás et al., 2004). In this sense, climatic conditions experienced during the cropping season are of special concern because of their direct impact on plant growth as well as their interannual and intraseasonal variability, which are expected to increase in the future in agreement with the rise in the frequency and intensity of extreme climate events (Magrin et al., 2014).

Photothermal conditions during the effective grain filling are usually subjected to a progressive deterioration under late sowing in temperate environments (Bonelli et al., 2016; Tsimba et al., 2013), as well as under several production systems at high latitude (Kiniry & Otegui, 2000; Tollenaar, 1983), mostly as a result of the decrease in solar radiation levels. Consequently, a reduction in final KW may occur as it has been documented for different maize kernel types grown under late sowing dates (Abdala et al., 2018; Bonelli et al., 2016; Cirilo et al., 2011). Disruptions in the photothermal environment during each subphase of grain filling were not addressed; such disruptions may cause an imbalance between the potential sink demand that is established early in kernel growth (Gambín et al., 2006) and the realization of this potential that takes place along active grain filling (Borrás et al., 2004).

Changes in source per grain around flowering affect the main physiological determinant of KW, namely the kernel growth rate (KGR) during the EGFP (Gambín et al., 2006). This rate is associated with the maximum kernel water content (KMWC; Borrás et al., 2003), which is achieved at mid-grain filling. The KMWC is considered a good estimator of the potential kernel size and can be used as an indirect estimate of kernel sink capacity (Borrás et al., 2003). Environmental limitations imposed during the EGFP affect KW directly, shortening the duration of this phase (Melchiori & Caviglia, 2008;

Core Ideas

- The increased kernel weight corresponded to the season with the highest photothermal records.
- Great photothermal imbalance between grain-filling phases resulted in reduced grain weight.
- Semidents had greater grain yield, kernel number, and plant growth around flowering than flints.
- Source–sink ratio at grain filling was lower for semident than for flint types.
- Semidents had increased kernel weight sensitivity to the photothermal environment.

NeSmith & Ritchie, 1992; Rattalino Edreira et al., 2014), mainly by accelerating kernel desiccation rate with almost no change in KGR (Jones & Simmons, 1983; Ouattar, Jones, & Crookston, 1987; Ouattar, Jones, Crookston, & Kajeiou, 1987; Westgate, 1994). A similar negative effect on grain-filling duration has been demonstrated for reduced irradiance with artificial shading (Andrade & Ferreiro, 1996). Such responses have not been documented through a wide range of natural environments for early-sown maize, which is assumed to be sink limited (i.e., to have source in excess for adequate completion of the grain-filling period) provided water and nutrients do not limit growth. Moreover, negative effects on grain filling may occur even under no soil resource limitations if above-optimum temperatures and/or high vapor pressure deficit limit transpiration (Shekoofa et al., 2016) and photosynthesis (Rotundo et al., 2019).

The sensitivity of individual KW to changes in the environment explored by crops during grain filling depends on the potential KW set early in grain development (sink strength) as well as on the source–sink relationship established subsequently during the effective grain filling (source capacity). Thus, genotypes that express a high potential KW and/or a constrained source–sink relationship during the EGFP will probably be more sensitive to variations in resource availability between early (i.e., *lag*) and late (i.e., effective) grain-filling phases than those expressing the opposite trend. Flint genotypes commonly have smaller KWs than dent germplasm because of a reduced potential KW that has been linked to a constrained plant growth around flowering (Tamagno et al., 2015). As a result of their reduced potential KW, flint genotypes are usually less affected than dents whenever source limitations are evident during grain filling (Tamagno et al., 2016), despite both groups have similar source–sink relationship at this period (Tamagno et al., 2015). More “modern” semident types showed greater KW reductions with severe defoliations

during seed filling than “old” flint genotypes when comparing Argentine hybrids released between 1965 and 1993 (Echarte et al., 2006). The same was evident when comparing modern flint and dent commercial hybrids (Tamagno et al., 2016), since dent types were more sensitive to the imposed source reductions per kernel during grain filling.

To our knowledge, there is no study that evaluates the impact of natural changes in the explored photothermal conditions at each phase of grain filling (*lag* and effective filling) on the KW, its physiological determinants (i.e., grain-filling traits), and the source–sink relationship during the post-flowering stages for genotypes of different genetic background (flint vs. semident germplasm). In current work we combined environmental characterization with crop physiology and genetic diversity to further our knowledge regarding both genetic responses to the environment and physiology underlying grain yield in maize. By doing so, the present study will evaluate for mentioned traits the effect of contrasting weather conditions (temperature, incident solar radiation, and vapor pressure deficit) during the LP, as well as the EGFP on a set of hybrids representative of dent \times flint (D \times F) and flint \times flint (F \times F) germplasm.

2 | MATERIALS AND METHODS

2.1 | Genetic material, crop husbandry, and experimental design

Field experiments were conducted at the Pergamino Experimental Station of the National Institute of Agricultural Technology (INTA), Argentina (33°56' S, 60°34' W), on a Typic Argiudoll soil during the growing seasons of 2002–2003 (Year 1, Y1), 2003–2004 (Year 2, Y2), 2013–2014 (Year 3, Y3), and 2014–2015 (Year 4, Y4). The evaluated genetic material included 12 single-cross hybrids derived from six inbred lines of different background. This background included one U.S. dent (B100), and five Argentine flint (LP2, LP561, LP611, LP662, and ZN6) inbreds described in detail in D'Andrea et al. (2006). The 12 hybrids were divided into two genotypic groups (GGs): (a) D \times F hybrids, composed by B100 \times LP2, B100 \times LP561, B100 \times ZN6, and their reciprocals; and (b) F \times F hybrids composed by LP561 \times LP662, LP561 \times LP611, LP611 \times ZN6, and their corresponding reciprocals. These types have been traditionally more widely used than pure dents in Argentina (Di Matteo et al., 2016; Echarte et al., 2006). Maize was hand planted on normal planting dates on 1 November (Y1), 9 October (Y2), 28 October (Y3), and 27 October (Y4). Soil analysis from the topmost 0.4 m of the soil profile indicated an organic matter content of 22 (Y1 and Y2), 23 (Y3), and 20 g kg⁻¹ (Y4). Nitrogen was applied at a rate of 200 kg N ha⁻¹ supplied as urea and split in two applications, one at sowing and another one at

the nine-ligulated leaf stage (V₉; Ritchie et al., 1992) reached at early (Y2) and mid-December (Y1, Y3, and Y4). Hybrids were distributed in a randomized complete block design with three replicates. Each experimental unit (plot) had three rows of 5.5-m length with a spacing of 0.7 m between rows. Stand density was always 7 plants m⁻². The uppermost 1 m of soil was kept near field capacity with sprinkler irrigation to prevent water stress. Weeds, insects, and diseases were controlled throughout the growing season.

2.2 | Measurements

Hourly recorded values of incident solar radiation and air temperature were obtained at the experimental site with a LI-COR 1200 (LI-COR) weather station. The fraction of incident radiation intercepted by the canopy was measured every 2 wk using a line quantum-sensor (Cavadevices). Four determinations per plot were taken at midday, between 1130 and 1430 h, on clear days, with 1 m of the sensor placed diagonally across the rows immediately below the lowermost green leaves of the canopy (Gallo & Daughtry, 1986). The duration of each evaluated growth stage was computed in cumulative thermal time units (TT, in °C d) above a base temperature of 8 °C and below an optimum temperature of 35 °C (Ritchie & NeSmith, 1991), except grain filling duration for which a base temperature of 0 °C was used (Muchow, 1990). A temperature of 35 °C was set for maximum records >35 °C, whereas no correction was made to minimum values because there was no record below 0 °C during grain filling.

Seven successive and well-bordered plants were tagged at V₃ on the central row of each plot. They were used for the nondestructive assessment of (a) the dates of anthesis (at least one anther visible in the tassel) and silking (at least one silk visible in the apical ear) of each plant, and (b) shoot biomass production per plant at V₁₄ (around silking –15 d) and R₂ (silking +15 d). These plants were harvested at physiological maturity (R₆; black layer visible in kernels at the middle of the ear) for the assessment of plant grain yield (PGY, in g plant⁻¹), kernel number per plant (KNP, counted for each ear of each plant), mean individual KW (KWm, as the quotient between PGY and KNP, in mg), and final shoot plant biomass (g plant⁻¹) after drying them at 70 °C until constant weight. Allometric models were used to estimate plant mass at V₁₄ and R₂ stages of crop development (Borrás & Otegui, 2001; Vega et al., 2000). Model predictors were (a) stem volume, based on the plant height to the uppermost visible collar and mean stem diameter at the base of the stalk (average of maximum and minimum values), for the estimation of vegetative biomass (i.e., excluding ear shoot); and (b) maximum ear diameter (only at R₂), for the estimation of ear–shoot biomass. Three or four plants per replicate were harvested for each genotype to parameterize

genotype-specific allometric models. All models were significant ($P < .001$), with r^2 values that ranged between .86 and .99 for vegetative biomass and .84 to .99 for ear–shoot biomass.

Additionally, during Y3 and Y4, 15 plants were randomly tagged 15 d before anthesis in each individual plot. Silking date (i.e., first silk visible) of the apical ear was recorded for all tagged plants. Individual kernel dry matter, and water content were measured throughout kernel development, beginning 10 d after silking until harvest maturity (~15% kernel moisture concentration) (Borrás et al., 2003). The apical ear of tagged plants was sampled every 4–6 d. The entire ear with surrounding husks was immediately enclosed in an airtight plastic bag and transported to the laboratory. Kernels were removed from the 10th (bottommost) spikelet position of the ear within a humidified box. Ten to fifteen kernels per ear were sampled on each date. Fresh weight was measured immediately after sampling, and kernel dry weight was determined after drying samples at 70 °C for at least 96 h. Fresh and dry weight data were used to calculate kernel water content (mg kernel^{-1}) throughout grain filling. Starting on 20 d after silking, 10 additional kernels were taken from each sampled ear for kernel volume determination by water volumetric displacement.

2.3 | Calculations

Weather variables records were computed for the LP and the EGFP. Mean air temperature (T) was obtained as the average of hourly recorded values. Daily vapor pressure deficit (VPD) was obtained as in Abbate et al. (2004). Mean incident radiation intercepted by the canopy (IRad) at each subphase of grain filling was estimated as the product between mean daily values of incident radiation (Rad) corresponding at each evaluated subphase (LP or EGFP) and fractional interception (fRad):

$$\text{IRad (MJ m}^{-2} \text{ d}^{-1}) = \text{Rad (MJ m}^{-2} \text{ d}^{-1}) \times \text{fRad} \quad (1)$$

Daily fractional interception values were obtained from nonlinear models fitted to observed data. The selection of the model in each year \times genotype \times replication combination was based on the r^2 value. The parameters of the selected models were fitted using the GraphPad Prism version 6.0 (Radushev, 2007) iterative optimization technique.

Two photothermal quotients were computed: the first (PTQ) as the ratio between Rad and T as in Equation 2, and the second (IPTQ) as the ratio between IRad and T as in Equation 3 (Fischer, 1985):

$$\text{PTQ (MJ m}^{-2} \text{ }^\circ\text{C}^{-1}) = \frac{\text{Rad (MJ m}^{-2} \text{ d}^{-1})}{T(^\circ\text{C})} \quad (2)$$

$$\text{IPTQ (MJ m}^{-2} \text{ }^\circ\text{C}^{-1}) = \frac{\text{IRad (MJ m}^{-2} \text{ d}^{-1})}{T(^\circ\text{C})} \quad (3)$$

The occurrence of LP and EGFP for each year of the historic climate series was estimated from mean TT values of LP and EGFP obtained as the average throughout evaluated genotypes and experiments, and based on a sowing date of 1 November. Then, T , Rad, IRad, VPD, PTQ, and IPTQ records of each year of the historical dataset were estimated for each evaluated grain filling subphase.

For each tagged plant, plant growth rate during the critical period (PGR_{CP}) was calculated as the ratio between plant biomass increase from V_{14} to R_2 and the TT interval between these sampling dates:

$$\text{PGR}_{\text{CP}} (\text{mg plant}^{-1} \text{ }^\circ\text{C d}^{-1}) = \frac{\text{biomass at } R_2 (\text{mg plant}^{-1}) - \text{biomass at } V_{14} (\text{mg plant}^{-1})}{\text{TT at } R_2 (\text{ }^\circ\text{C d}) - \text{TT at } V_{14} (\text{ }^\circ\text{C d})} \quad (4)$$

Plant growth rate per kernel during the critical period ($\text{PGR}_{\text{CP}} \text{ kernel}^{-1}$) was obtained as the quotient between PGR_{CP} and KNP:

$$\text{PGR}_{\text{CP}} \text{ kernel}^{-1} (\text{mg }^\circ\text{C d}^{-1} \text{ kernel}^{-1}) = \frac{\text{PGR}_{\text{CP}} (\text{mg plant}^{-1} \text{ }^\circ\text{C d}^{-1})}{\text{KNP (kernels plant}^{-1})} \quad (5)$$

Plant growth during the EGFP (PG_{EGFP}) was obtained as shoot biomass increase from R_2 up to R_6 :

$$\text{PG}_{\text{EGFP}} (\text{g plant}^{-1}) = \text{biomass at } R_6 (\text{g plant}^{-1}) - \text{biomass at } R_2 (\text{g plant}^{-1}) \quad (6)$$

Plant growth per kernel during the EGFP ($\text{PG}_{\text{EGFP}} \text{ kernel}^{-1}$) was obtained as the quotient between PG_{EGFP} and KNP:

$$\text{PG}_{\text{EGFP}} \text{ kernel}^{-1} (\text{mg kernel}^{-1}) = \frac{\text{PG}_{\text{EGFP}} (\text{mg plant}^{-1})}{\text{KNP (kernels plant}^{-1})} \quad (7)$$

Kernel weight, KGR, and duration of the EGFP of each hybrid \times replicate \times year combination were estimated by a bilinear model (Equations 8 and 9) fitted to each dataset (Borrás & Otegui, 2001):

$$\text{KWe} = a + b \text{ TT} \quad \text{for } \text{TT} \leq c \quad (8)$$

$$\text{KWe} = a + bc \quad \text{for } \text{TT} > c \quad (9)$$

where KWe is the estimated kernel dry weight (mg kernel^{-1}), TT the thermal time after silking ($^\circ\text{C d}$), a the y intercept

(mg kernel⁻¹), b is the KGR during the EGFP (mg kernel⁻¹ °C d⁻¹), and c is the total grain-filling duration (°C d). The duration of the EGFP was estimated as the difference between the total grain-filling duration and the TT when KWe = 0.

A bilinear model was also used for the estimation of maximum kernel volume (KMV):

$$KV = d + e TT \quad \text{for } TT \leq f \quad (10)$$

$$KV = d + ef \quad \text{for } TT > f \quad (11)$$

where KV is the kernel volume (μl kernel⁻¹), TT is the thermal time after silking (°C d), d is the y intercept (μl kernel⁻¹), e is the rate of kernel volume increase (μl kernel⁻¹ °C d⁻¹), and f is the period of kernel volume increase (°C d).

The KMWC was estimated by fitting a trilinear model (Gambín et al., 2007):

$$WC = g + h TT \quad \text{for } TT \leq i \quad (12)$$

$$WC = g + hi + j(TT - i) \quad \text{for } TT > i \text{ and } TT < k \quad (13)$$

$$WC = g + hi + j(k - i) - l(TT - k) \quad \text{for } TT \geq k \quad (14)$$

where WC is the water content (mg kernel⁻¹), TT is the thermal time after silking, g is the y intercept (mg kernel⁻¹), h is the initial rate of kernel water accumulation (mg kernel⁻¹ °C d⁻¹), i is the TT at which a shift in the rate of water content increase is detected (°C d), j is the rate of kernel water accumulation during the second phase (mg kernel⁻¹ °C d⁻¹), k is the TT at maximum water content (°C d), and l is the rate of water loss from maximum water content to physiological maturity (mg kernel⁻¹ °C d⁻¹).

Nonlinear models were fitted for each year × genotype × replication combination using the GraphPad Prism version 6.0 (Raduschev, 2007) iterative optimization technique.

2.4 | Statistical analysis

For each trait, statistical analysis was performed using linear-mixed effect models in R 3.4.1 (R Core Team, 2018; lme4 package, lmer function). Experimental year (Y) and genotypic group (GG) were included in the model as fixed effects, whereas block and hybrid were considered random effects as follows:

$$Y_{ijkl} = \mu + \alpha_i + \beta_j (\alpha_i) + \gamma_k + \alpha_i \gamma_k + \rho_{ijk} + \delta_l (\gamma_k) + \varepsilon_{ijkl} \quad (15)$$

where Y_{ijkl} is the trait value of the i th year ($i = 4$), the j th block ($j = 3$), the k th genotypic group ($k = 2$), and the l th hybrid ($l = 12$); μ the overall mean; α_i the year effect; $\beta_j(\alpha_i)$ the block effect; nested within each experimental year; γ_k the genotypic group effect; $\alpha_i \gamma_k$ is the interaction effect between the year and the genotypic group; ρ_{ijk} is the error of the main plot; $\delta_l(\gamma_k)$ the hybrid effect nested within genotypic group; and ε_{ijkl} is the random residual effect. Statistical differences for the significant sources of variation were tested using LSD at the 5% level.

Two principal components analyses (PCA) were performed on the hybrid × attribute matrix containing standardized data. Hybrids were grouped by the genotypic group and the year. The first PCA included grain yield and its components, plant growth, and source–sink relationships during reproductive stages, whereas the second PCA included the KWe and grain-filling traits. Additionally, the first PCA included climatic variables as supplementary variables. These variables were not used for the determination of the principal components, and their coordinates were predicted using only the information provided by the performed PCA on active variables and individuals. The results of the two ordination analysis were presented in two different biplots. Both biplots were constructed using the first two principal components (PC1 and PC2) to determine the relationships among traits, hybrids, and climatic variables. Only the first two PCs were considered because they explained a large proportion (~80%) of the total explored variability. The analysis was performed using factoextra (version 1.0.5) and factoMineR (version 2.3) packages in R 3.4.1 (R Core Team, 2018).

3 | RESULTS

3.1 | Weather conditions

Meteorological conditions were considerably different among experimental years (Table 1, Figure 1) not only during the LP, but also during the effective grain filling. During the LP, Y3 had the highest records for all evaluated weather variables (in bold, Table 1), except for the PTQ; the opposite trend was observed in Y4 (Table 1). Moreover, for both mean air temperature and mean incident solar radiation, Y3 and Y4 records were located in the uppermost (>75th percentile) and the lowermost (<25th percentile) part of the frequency distribution, respectively (Figures 1a and 1c). The other two growing seasons also corresponded to the extreme quartiles of mean air temperature during the LP, being Y1 high and Y2 low (Figure 1). Y3 records during the LP were ~25% higher than Y2 for mean temperature, and ~40% and 20% higher than Y4 for vapor pressure deficit (VPD) and incident solar radiation, respectively (Table 1). In addition, 40% of the Y3 LP (5 d)

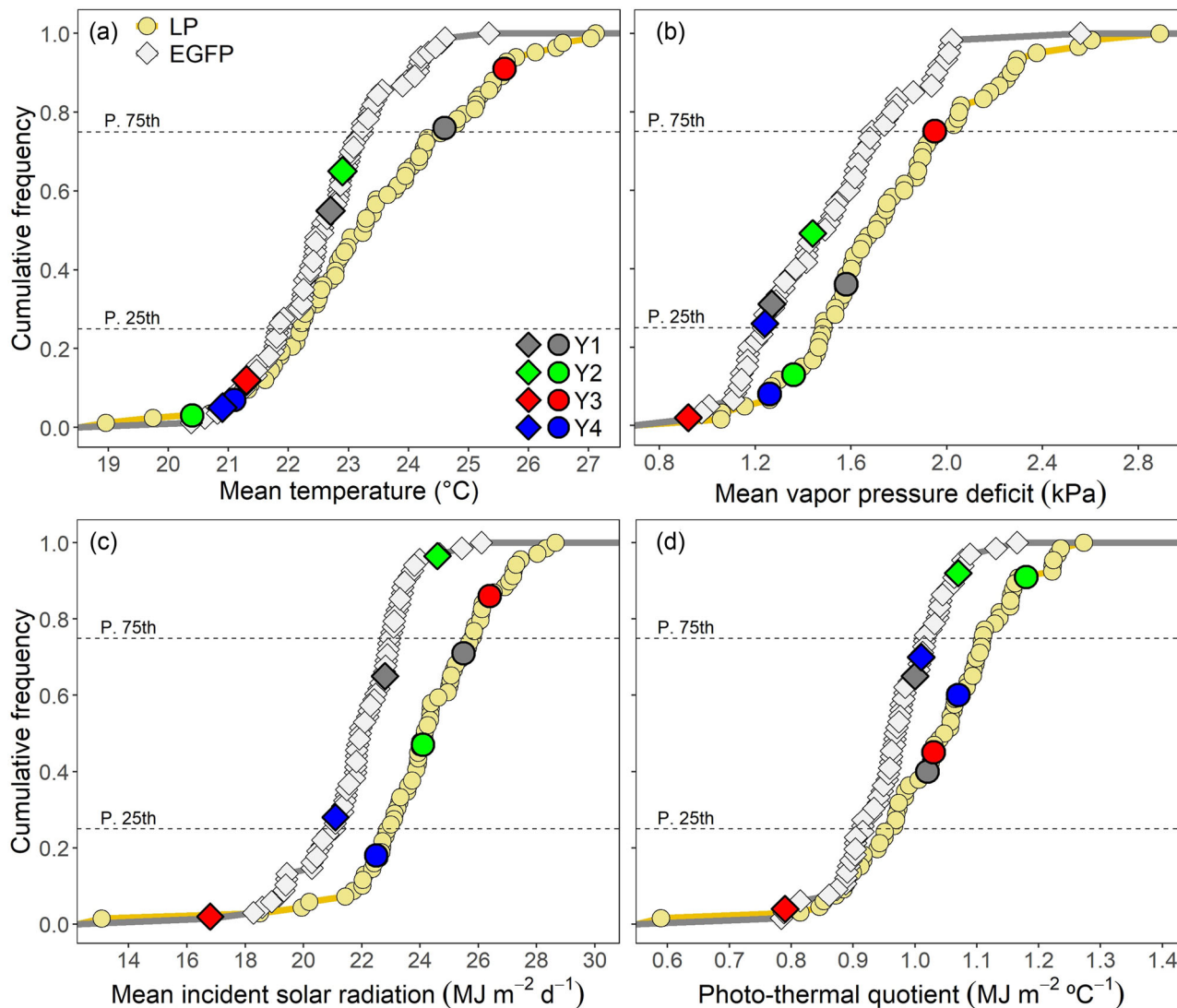


FIGURE 1 Cumulative frequency for (a) daily mean air temperature, (b) mean vapor pressure deficit, (c) mean incident solar radiation, and (d) photothermal quotient on incident solar radiation basis during the *lag* phase (LP, in yellow) and the effective grain-filling period (EGFP, in gray). Data correspond to the historical meteorological datasets recorded at the Pergamino Experimental Station for a sowing date of 1 November. The mean extension of *lag* and EGFP were computed across all genotypes and experiments of current research. For each variable, values for Years 1 (2002–2003, Y1), 2 (2003–2004, Y2), 3 (2013–2014, Y3), and 4 (2014–2015, Y4) are indicated in different colors

had maximum temperature values above 35 °C (Supplemental Figure S1).

During the EGFP, Y2 had the highest records of mean temperature, VPD, and solar radiation (in bold, Table 1), and for incident radiation, this year was located at the top of the frequency distribution (90th percentile; Figure 1c). By contrast, Y3 exhibited the lowest values during the EGFP for all evaluated variables, particularly for VPD (36% smaller than Y2) and incident solar radiation (32% smaller than Y2) as a result of a high proportion of cloudy days. Moreover, Y3 corresponded to the lowermost part (<20th percentile) of the frequency distribution (Figures 1a, b, c). In addition, Y3 recorded a large decline between both grain-filling phases for

VPD as well as for incident and intercepted solar radiation (Var. in Table 1).

As a consequence of the described irradiance and temperature combinations of Y2 (higher irradiance than temperature during the LP and the EGFP; Figures 1a and 1c), its PTQs were the highest in both subphases of grain filling (Table 1, Figure 1d). By contrast, the PTQ and IPTQ during the EGFP in Y3 were substantially lower than in the other analyzed experiments and recorded a large decline in comparison with the LP (Var. in Table 1). Thus, Y3 was classified near the historical mean for the PTQ during the LP but ranked the second lowermost historical value of the analyzed series for the EGFP (Figure 1d).

TABLE 1 Average climatic data during the lag phase (LP) and the effective grain-filling period (EGFP), and the percentage of variation {Var. = [(EGFP – LP) × 100]/LP} for experiments developed during 2002–2003 (Y1), 2003–2004 (Y2), 2013–2014 (Y3), and 2014–2015 (Y4) seasons. Historical (H) data (1932–2018 for temperature and 1949–2018 for the rest) at the Pergamino site for a sowing date of 1 November are indicated as reference

Year	Mean temperature			Vapor pressure deficit			Incident solar radiation			Intercepted solar radiation			Photothermal quotient ^a					
	LP	EGFP	Var.	LP	EGFP	Var.	LP	EGFP	Var.	LP	EGFP	Var.	LP	EGFP	Var.			
	°C			kPa			MJ m ⁻² d ⁻¹			MJ m ⁻² d ⁻¹			MJ m ⁻² °C ⁻¹					
Y1	24.6	22.7	-7.7	1.58	1.27	-20	25.5	22.8	-10	24.1	18.5	-23	1.02	1.00	-0.03	0.98	0.81	-17
Y2	20.4	22.9	12	1.36	1.44	5.9	24.1	24.6	2.1	22.1	20.6	-6.8	1.18	1.07	-9.3	1.08	0.90	-17
Y3	25.6	21.3	-17	1.95	0.92	-53	26.4	16.8	-36	22.1	15.2	-31	1.03	0.79	-23	0.86	0.71	-17
Y4	21.1	20.9	-0.9	1.29	1.28	-1.6	22.5	21.1	-6.2	17.9	16.7	-6.7	1.07	1.01	-5.6	0.84	0.79	-6.0
H	23.4	22.8	-2.6	1.77	1.50	-15	23.8	22.6	-5.0	-	-	-	1.01	0.98	-3.0	-	-	-

^aPhotothermal quotient and IPhotothermal quotient were computed on incident and intercepted solar radiation basis, respectively.

3.2 | Kernel weight, plant growth, and source–sink relationship

All traits had a significant ($P < .05$) Y and GG effect (Table 2); however, a significant Y × GG interaction was detected for PGR_{CP} kernel⁻¹, KWm, KNP, and PGY. Among experimental years, the highest mean values for PGY and yield components (i.e., KNP and KWm) corresponded to Y2 and Y4, which also had the greatest values for most plant growth traits and the source–sink relationships (Table 2). By contrast, the most unfavorable season in terms of the explored photothermal conditions (Y3) had the lowest values for PGY and most evaluated traits; this year also exhibited a more pronounced decrease in KWm than in KNP as compared with the rest of years (Table 2).

Regarding genotypic groups, D × F hybrids had larger ($P < .01$) mean values for PGY and its components (KNP and KWm) than F × F types (Table 2), and despite the presence of significant Y × GG interaction for mentioned traits, D × F superiority for PGY and KNP held across all evaluated years (Table 3). The same response pattern was observed for plant growth during the critical period (Table 3). The F × F group was superior ($P < .05$) for mean values of plant growth and source–sink ratio during the EGFP, not only when averaged across experimental years (Table 2), but also at each evaluated season (Table 3). When extreme values across years were considered, the highest range (Table 3) corresponded to D × F hybrids, except for minimum records of KNP and PGY and maximum records of PG_{EGFP} kernel⁻¹. Similarly, D × F exhibited larger interannual variability than F × F in mean values of all evaluated traits (SE in Table 3), particularly PGY, KNP, and KWm.

3.3 | Environment × trait × genotypic group associations

A PCA was used to evaluate the relationships among attributes, weather conditions, and genotypic groups. The first two components (PC1 and PC2) accounted for 78% of the observed variation (Figure 2). Most part of the climatic effects was explained by the PC1, whereas the contrast between genotypic groups was sorted by the PC2. Though PGY was mainly associated with the variation observed in KNP along the PC2, part of PGY variation was also explained by the variation in KWm along the PC1 (Figure 2). The KWm was positively and strongly associated with PG_{EGFP} and with both source–sink ratios, which in turn were positively associated with their corresponding plant growth traits. The KNP was mainly linked to PGR_{CP} and had no relation with KWm, though KWm was also related to PGR_{CP} .

TABLE 2 Mean \pm standard error values for fixed factors year (Y) and genotypic group (GG) (top), and ANOVA results (bottom). Data correspond to experiments developed during 2002–2003 (Y1), 2003–2004 (Y2), 2013–2014 (Y3), and 2014–2015 (Y4) growing seasons. The greatest value of each trait is bolded

Source of variation	df ^a	PGR _{CP} mg plant ⁻¹ °C d ⁻¹	PGR _{CP} kernel ⁻¹ mg °C d ⁻¹ kernel ⁻¹	PG _{EGFP} g plant ⁻¹	PG _{EGFP} kernel ⁻¹ mg kernel ⁻¹	KWm mg kernel ⁻¹	KNP kernels plant ⁻¹	PGY g plant ⁻¹
Year								
Y1		261 \pm 4.8b ^b	0.58 \pm 0.01	127 \pm 3.1a	280 \pm 6.7a	279 \pm 3.6	456 \pm 6.6	127 \pm 1.8
Y2		333 \pm 7.2a	0.69 \pm 0.02	133 \pm 4.2a	278 \pm 9.9a	286 \pm 3.1	484 \pm 7.7	138 \pm 2.5
Y3		228 \pm 6.1c	0.48 \pm 0.01	98 \pm 2.8b	210 \pm 6.7b	252 \pm 2.7	474 \pm 9.0	118 \pm 2.0
Y4		321 \pm 7.7a	0.62 \pm 0.01	134 \pm 3.9a	269 \pm 8.5a	282 \pm 3.0	506 \pm 13	142 \pm 3.8
Genotypic group								
D \times F		303 \pm 6.9a	0.59 \pm 0.01	118 \pm 3.1b	236 \pm 6.1b	276 \pm 3.2	507 \pm 7.3	139 \pm 2.2
F \times F		269 \pm 6.2b	0.60 \pm 0.01	128 \pm 2.8a	283 \pm 5.9a	272 \pm 2.0	453 \pm 5.4	123 \pm 1.7
ANOVA								
Y	3	***	***	***	***	***	***	***
GG	1	**	*	*	*	**	**	**
Y \times GG	3	ns ^c	**	ns	ns	***	***	**

Note. D \times F, dent by flint; F \times F, flint by flint; KNP, kernel number per plant; KWm, mean kernel weight; PG_{EGFP}, plant growth during the effective grain-filling period; PG_{EGFP} kernel⁻¹, PG_{EGFP} per kernel; PGR_{CP}, plant growth rate during the critical period for kernel set; PGR_{CP} kernel⁻¹, PGR_{CP} per kernel; PGY, plant grain yield.

^aNo shared letter within a column and source of variation represents significant differences at $P < .05$.

*Significant at the .05 probability level.

**Significant at the .01 probability level.

***Significant at the .001 probability level.

^cns, nonsignificant.

TABLE 3 Mean values \pm standard error of evaluated traits for dent by flint ($D \times F$) and flint by flint ($F \times F$) hybrids at each experimental year. Data correspond to experiments developed during 2002–2003 (Y1), 2003–2004 (Y2), 2013–2014 (Y3), and 2014–2015 (Y4) growing seasons. The greatest value of each trait is bolded. Trait description as in Table 2

Trait	GG ^a	Y1	Y2	Y3	Y4	Range ^b	SE
PGR _{CP} , mg plant ⁻¹ °C d ⁻¹	D × F	277 \pm 5.6	343 \pm 9.5	241 \pm 9.7	349 \pm 10	164–434	26.2
	F × F	245 \pm 5.8	322 \pm 10	215 \pm 6.2	294 \pm 6.7	167–383	24.0
PGR _{CP} kernel ⁻¹ , mg °C d ⁻¹ kernel ⁻¹	D × F	0.61 \pm 0.02	0.70 \pm 0.03	0.46 \pm 0.01	0.63 \pm 0.02	0.32–0.94	0.050
	F × F	0.56 \pm 0.02	0.68 \pm 0.02	0.50 \pm 0.01	0.67 \pm 0.02	0.40–0.89	0.045
PG _{EGFP} , g plant ⁻¹	D × F	120 \pm 3.4	127 \pm 6.3	90 \pm 2.7	134 \pm 6.4	70–183	9.7
	F × F	134 \pm 4.7	139 \pm 5.5	106 \pm 4.2	133 \pm 4.7	73–177	7.6
PG _{EGFP} kernel ⁻¹ , mg kernel ⁻¹	D × F	265 \pm 9.7	258 \pm 12	181 \pm 4.8	238 \pm 10	138–348	19.0
	F × F	294 \pm 8.1	297 \pm 14	239 \pm 7.8	300 \pm 9.3	184–414	14.6
KWm, mg kernel ⁻¹	D × F	293 \pm 4.9	293 \pm 4.8	241 \pm 2.6	279 \pm 3.5	221–323	12.5
	F × F	265 \pm 2.4	279 \pm 3.2	263 \pm 2.9	285 \pm 4.8	241–322	5.4
KNP, kernels plant ⁻¹	D × F	458 \pm 7.8	493 \pm 11	509 \pm 9.7	567 \pm 14	373–776	22.7
	F × F	455 \pm 10	474 \pm 9.9	439 \pm 9.6	444 \pm 11	368–554	8.1
PGY, g plant ⁻¹	D × F	133 \pm 2.1	144 \pm 3.4	122 \pm 2.8	157 \pm 4.3	96–207	7.5
	F × F	120 \pm 2.2	132 \pm 3.1	114 \pm 2.8	126 \pm 3.7	90–159	3.9

^aGG, genotypic group.

^bRange is from minimum to maximum values.

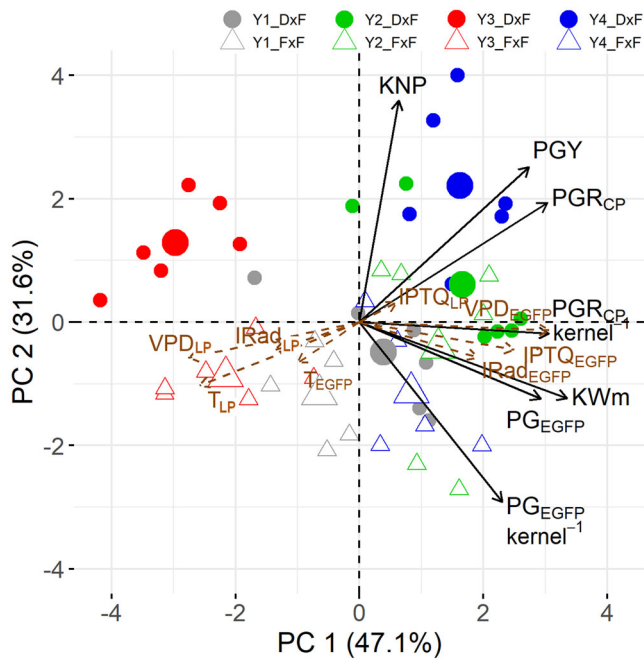


FIGURE 2 Biplot for the first two principal components (PC 1 and PC 2) of 12 hybrids evaluated during four experimental years (2002–2003, Y1; 2003–2004, Y2; 2013–2014, Y3; 2014–2015, Y4) for attributes of plant growth, source–sink relationship during reproductive stages, grain yield, and its components. Traits and meteorological variables are represented by black solid and brown dashed vectors, respectively. Genotypes of two groups (D × F: dent by flint; F × F: flint by flint) are indicated by different symbols. The enlarged symbols represent the mean value for each genotypic group (GG) × year (Y) combination. IPTQ_{EGFP}, photothermal quotient on intercepted solar radiation basis during the effective grain-filling period; IPTQ_{LP}, IPTQ during the lag phase; IRad_{EGFP}, mean intercepted solar radiation during the effective grain-filling period; IRad_{LP}, IRad during the lag phase; KNP, kernel number per plant; KWM, mean kernel weight; PG_{EGFP}, plant growth during the effective grain-filling period; PG_{EGFP} kernel⁻¹, PG_{EGFP} per kernel; PGR_{CP}, plant growth rate during the critical period for kernel set; PGR_{CP} kernel⁻¹, PGR_{CP} per kernel; PGY, plant grain yield; T_{EGFP}, daily mean temperature during the effective grain-filling period; T_{LP}, T during the lag phase; VPD_{EGFP}, vapor pressure deficit during the effective grain-filling period; VPD_{LP}, VPD during the lag phase

Regarding the relationship between evaluated traits and weather variables, KWM was strongly and positively associated with the amount of intercepted solar radiation and the PTQ during the effective grain filling (i.e., IRad_{EGFP} and IPTQ_{EGFP}), and to a lesser extent with vapor pressure deficit at the same period (VPD_{EGFP}) and photothermal conditions during the LP (IPTQ_{LP}). The IPTQ_{LP} was closely and positively associated with PGR_{CP}, PGY, and KNP. By contrast, mean air temperature, VPD, and intercepted solar radiation during the LP (T_{LP}, VPD_{LP}, and IRad_{LP}), along with mean temperature during the effective grain filling (T_{EGFP})

integrated the group of weather variables that were negatively associated with most of the analyzed traits (Figure 2).

Marked differences among years as well as between genotypic groups in their respective spatial ordination patterns were detected (Figure 2). As already mentioned, genotypic groups tended to be sorted across the PC2 (D × F to the upper half and F × F to the bottom half), whereas experimental years were predominantly sorted across the PC1. The D × F genotypes tended, on average, towards increased KNP, PGY and PGR_{CP} (mainly for Y2 and Y4). The F × F types usually highlighted for PG_{EGFP} and particularly for PG_{EGFP} kernel⁻¹, since they intercepted mentioned traits on its positive sense (except in Y3, Figure 2). Regarding experimental years, hybrids during Y2 and Y4 were grouped, on average, towards high KWM (projection on the positive sense of the KWM vector) as well as high KNP (only for D × F types). It is worth noting the trend observed for Y3, with lowest values for most traits except for KNP among D × F genotypes (Figure 2).

3.4 | Kernel weight determination by the source–sink relations in response to changes in the environment

Mean KW (KWM) was associated with variations in both source–sink ratios (Figures 2 and 3), although stronger for D × F than for F × F types (Figures 3b and 3c), whereas KNP slightly responded to the large variation in PGR_{CP} and only for D × F (Figure 3a).

For the response of the KWM to the source–sink relationship during the critical period (PGR_{CP} kernel⁻¹), two bilinear with plateau models were separately fitted ($P < .01$) for each genotypic group (Figure 3b), since fit to each data set differed ($P < .01$) from each other. The D × F hybrids exceeded F × F not only in the response of KWM to PGR_{CP} kernel⁻¹ at KWM values below the plateau (311 ± 48 vs. 177 ± 63 °C d) but also in the threshold to achieve maximum KWM (0.63 ± 0.02 vs. 0.60 ± 0.04 mg °C d⁻¹ kernel⁻¹) as well as in the maximum estimated KWM (294 ± 27 vs. 280 ± 35 mg). By contrast, the F × F group was superior in the minimum attainable KWM when no plant growth per kernel is detected (174 ± 27 vs. 97.8 ± 32 mg).

For the response of the KWM to the source–sink relationship during the effective grain filling (PG_{EGFP} kernel⁻¹), two bilinear with plateau models were separately fitted ($P < .001$) for D × F and F × F types (Figure 3c), but a more robust fit was obtained for the former ($r^2 = .83$; $P < .001$) than for the latter ($r^2 = .30$; $P < .01$). The D × F hybrids considerably overcame F × F in the KWM response to the increase in PG_{EGFP} kernel⁻¹ (0.60 ± 0.08 vs. 0.18 ± 0.08), and in the maximum KWM estimated by the model (299 ± 18 vs. 282 ± 27 mg), whereas the F × F group was superior in the minimum

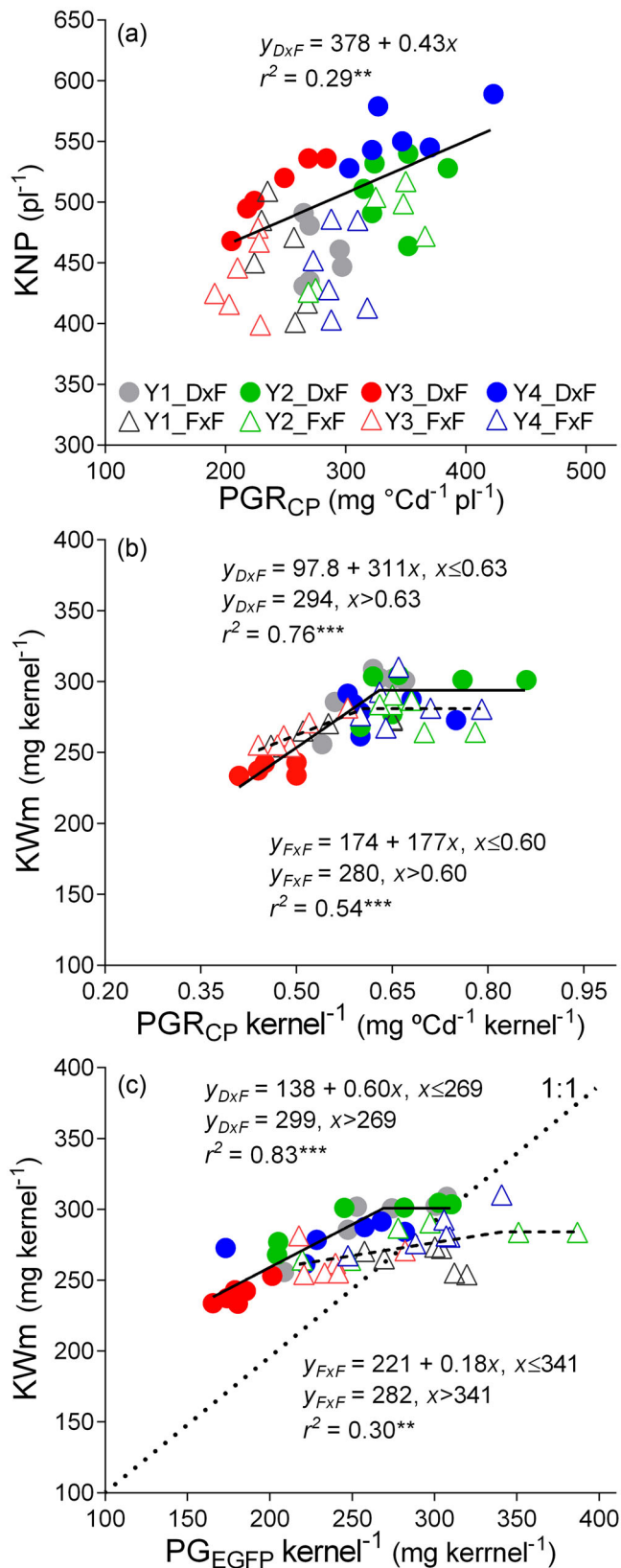


FIGURE 3 Response of (a) kernel number per plant (KNP) to plant growth rate during the critical period (PGR_{CP}), (b) mean kernel weight (KWm) to PGR_{CP} per kernel ($PGR_{CP} \text{ kernel}^{-1}$), and (c) KWm to plant growth per kernel during the effective grain-filling period ($PG_{EGFP} \text{ kernel}^{-1}$) for 12 hybrids evaluated during four experimental years (2002–2003, Y1; 2003–2004, Y2; 2013–2014, Y3; 2014–2015,

attainable KWm when no $PG_{EGFP} \text{ kernel}^{-1}$ is detected (221 ± 22 vs. 138 ± 17 mg). Likewise, all D \times F points were above the 1:1 relationship, whereas a considerable proportion of F \times F data ($\sim 50\%$) was to the right of the 1:1 relationship. The former is indicative of apparent reserves use for grain filling whereas the latter is indicative of an excess of source to fulfill kernels.

Among evaluated seasons, points representative of Y3 were located at the lowest source–sink ratio levels (leftmost side of the x axis), whereas the rest of the years experienced improved ratios, including data at the plateau of the fitted models (Figures 3b and 3c). Consequently, the magnitude of the decrease in both source–sink ratios ($PGR_{CP} \text{ kernel}^{-1}$, $PG_{EGFP} \text{ kernel}^{-1}$) was remarkable in Y3 (around -25%) respect to the average of the other evaluated years (Figure 4). A similar trend, but of reduced magnitude ($\sim 12\%$), was observed for KWm. The extent of mentioned reductions was substantially higher among D \times F than among F \times F types, mostly for KWm, which was constrained more than three times in the former (17%) with respect to the latter (5%). Likewise, important differences were detected between groups in the relative reduction (Figure 4) computed for $PG_{EGFP} \text{ kernel}^{-1}$ (D \times F, -30% vs. F \times F, -19%), and $PGR_{CP} \text{ kernel}^{-1}$ (D \times F, -29% vs. F \times F, -21%).

3.5 | Kernel weight and its physiological components: Responses to the environment

When the physiological determinants of KW were analyzed during Y3 and Y4, important ($P < .05$) differences between seasons were detected for estimated KW (KWe), KMW, and KGR; however, mentioned differences depended upon the genotypic group considered (significant Y \times GG interaction; Supplemental Table S1).

The PCA analysis shows KWe was positively associated with KMW and KMW, and to a lesser extent with KGR (Figure 5). There was no relation between KWe and the duration of the EGFP, and this trait did not vary ($P > .05$) with the different years and genotypic groups (Supplemental Table S1). Regarding both main KWe components (i.e., KGR and EGFP), they were negatively associated with each other (Figure 5).

Experimental years were consistently sorted along the PC1, with red symbols to the left for Y3 and blue symbols to the right for Y4 (Figure 5). This component explained by itself a

Y4). A single linear model fitted the whole data set of dent by flint (D \times F) genotypes (solid line, $n = 24$, $P < .01$) in Panel a, whereas a single bilinear with plateau model fitted the whole data set of D \times F (solid line, $n = 24$, $P < .001$) and flint by flint (F \times F, dashed line, $n = 24$, $P < .01$) genotypes in Panels b and c. The dotted line in Panel c represents the 1:1 relationship

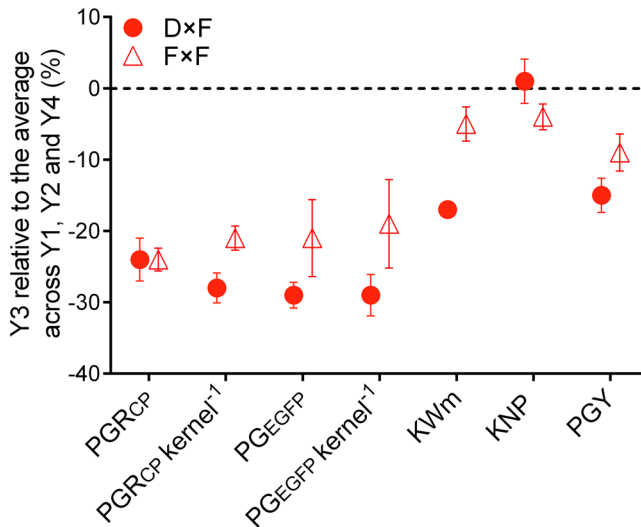


FIGURE 4 Relative decrease in Year 3 (Y3) to the average value across the rest of the evaluated years (Y1, Y2, and Y4) for attributes of plant growth, source–sink relationships during reproductive stages, and grain yield and its components for dent \times flint (D \times F) and flint \times flint (F \times F) hybrids. Years 1, 2, 3, and 4 correspond to experiments developed during 2002–2003, 2003–2004, 2013–2014, and 2014–2015 growing seasons, respectively. Vertical lines represent the standard error of the mean. Trait description as in Figure 2

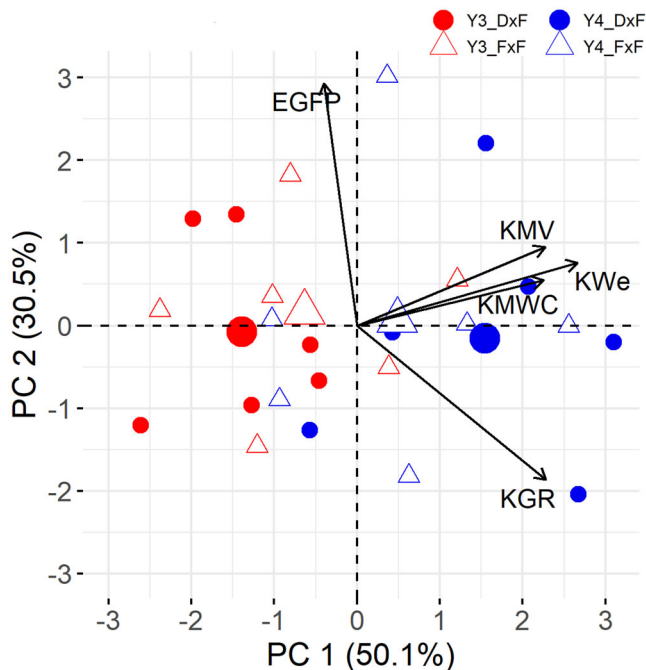


FIGURE 5 Biplot for the first two principal components (PC 1 and PC 2) of 12 hybrids evaluated during two experimental years (2013–2014, Y3; 2014–2015, Y4) for estimated KW (KWe) and its physiological components. Genotypes of two groups (D \times F: dent by flint; F \times F: flint by flint) are indicated by different symbols. The enlarged symbols represent the mean value for each genotypic group (GG) \times year (Y) combination. EGFP, effective grain-filling period; KGR, kernel growth rate; KMV, maximum kernel volume; KMWC, maximum kernel water content

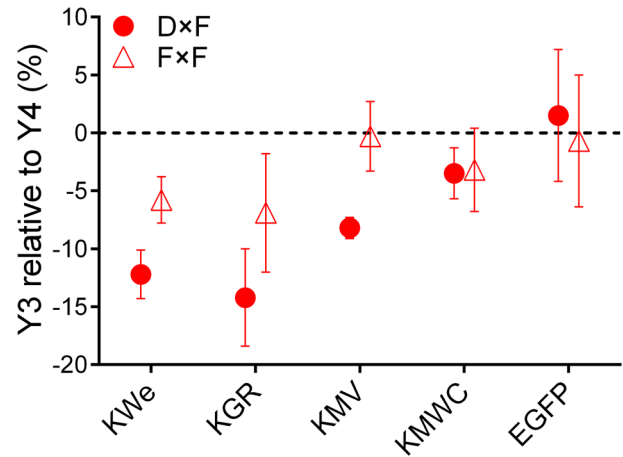


FIGURE 6 Mean relative values for estimated kernel weight (KWe) and its physiological components corresponding to dent by flint (D \times F) and flint by flint (F \times F) hybrids. Years 3 and 4 correspond to experiments developed during 2013–2014 and 2014–2015 growing seasons, respectively. Vertical lines correspond to standard error of mean. EGFP, effective grain-filling period; KGR, kernel growth rate; KMV, maximum kernel volume; KMWC, maximum kernel water content

half of the total variation. In this sense, trait vectors had positive trajectories to the right of PC1 (except EGFP), in concordance with the highest average records for most traits in Y4 (Figure 6). However, differences between years were greater for D \times F than for F \times F types, as the former were located, on average, closer to the extremes along the PC1 than the latter (Figure 5). This was evident for KWe, KGR, and KMV, which were considerably ($P < .05$) constrained in D \times F in comparison with F \times F hybrids at Y3 (Figure 6).

4 | DISCUSSION

In this work, we evaluated the response of hybrids representative of two genotypic backgrounds (D \times F and F \times F germplasm) to natural changes in the environment that occurred during each subphase of grain filling (LP and EGFP). Our analytical framework combined environmental characterization with crop physiology and genetic diversity, highlighting the dependency of KW and its components upon the environment and the genetic background. The experimental approach enabled us to investigate this dependency within the experimental limitations of continuous processes (Messina et al., 2019), as in the case of both interrelated grain filling subphases that together integrate the whole grain-filling period. The explored environmental variation included (a) two growing seasons (Y1 and Y4) with a photothermal environment (i.e., PTQ) close to mean historical records for both grain filling subphases, (b) one season (Y2) with above-average PTQ in both subphases, and (c) one season (Y3) with

contrasting PTQ between subphases. The latter corresponded to 21% of the years for the analyzed series in the region under study (lowermost right quadrant in Supplemental Figure S2). Similar climatic variations than those observed in current research are ensured in breeding programs by means of the so-called “managed-environments” rather than by including more years and locations in the same region (Cooper et al., 1995; de la Vega & Chapman, 2001).

4.1 | Kernel weight and its related traits, plant growth, and source–sink relationship in response to the photothermal conditions

Maize KW was strongly affected by weather conditions explored during grain filling, expressing a considerable reduction in Y3, which had the smallest PTQs during the period of potential KW determination and during the effective filling period (Table 1, Figure 1). By contrast, Y2 obtained the highest KW, in agreement with the most favorable photothermal environments explored at both subphases of grain filling. Differences in photothermal conditions among experimental years tended to be larger during the effective grain filling than during the LP (PTQ_{EGFP} and IPTQ_{EGFP} markedly differed between Y2 and Y3). Considering both climatic components of the PTQ (i.e., solar radiation and mean temperature), their relative impact varied between grain-filling phases.

During the LP, mean temperatures under the prevalent near-optimum temperature records in Y3 had a negative effect on grain growth processes, because such conditions represent the maximum developmental rate and consequently the minimum phase duration (Ritchie & NeSmith, 1991). This may have negatively affected overall assimilates production and potential KW (Capitanio et al., 1983). High mean and maximum (larger than 35 °C) temperatures during Y3 LP did not seem to be high enough to increase ear temperature up to levels conducive to kernel abortion (i.e., direct effect of heat stress on kernel set). However, such temperatures along with high VPD records in Y3 did produce a decline in PGR_{CP}, probably associated with a decrease in radiation use efficiency (Cicchino et al., 2010; Rattalino Edreira & Otegui, 2012; Stockle & Kiniry, 1990; Wahid et al., 2007), affecting the potential KW determination because of source limitations (Figures 3b and 4). On the one hand, described temperature gradients are frequent across maize canopies exposed to above-optimum temperatures (Rattalino Edreira & Otegui, 2012), being larger in the uppermost organs (i.e., tassel, uppermost leaves) than in the lowermost ones. This turned out in a variable incidence of described effects depending upon temperature rise at the individual organ level. On the other hand, described temperature effects were not correctly assessed by a simple PTQ of the type used to predict kernel number in a winter cereal as wheat (Fischer, 1985), for which the chance

in the occurrence of supra-optimum temperatures is usually negligible. By contrast, in summer crops, the use of the PTQ should be taken carefully because heat stress episodes are frequent during the cycle, particularly during reproductive stages.

In contrast to temperature, incident solar radiation may have had a preponderant influence during the EGFP (Bonelli et al., 2016; Cirilo & Andrade, 1996), since the PTQ_{EGFP} decrease recorded in Y3 could be attributed to the great reduction in incident solar radiation levels rather than to differences among evaluated years in mean air temperature or in VPD_{EGFP} (Table 1, Figure 1). Under early sowing at intermediate latitudes, as in the current research, the LP usually develops under maximum incident solar radiation levels and high temperatures (Bonelli et al., 2016; Maddonni, 2012). In this phase, in which potential KW as well as KGR are established, the probability of negative effects associated with above-optimum temperatures is more critical than the potential reduction in solar radiation (Maddonni, 2012). As the grain-filling stage progresses, the decrease in solar radiation levels becomes more evident, as usually reported for high latitude environments (Tollenaar, 1983) and late sowings in intermediate latitudes (Bonelli et al., 2016; Maddonni, 2012). Thus, prolonged cloudy events during the effective grain filling are expected to be critical for final KW determination, mainly because of the reduction in the plant capacity (i.e., source activity) to fulfill the high assimilates demand (i.e., sink strength) established previously during the critical period (Borrás et al., 2004), as demonstrated by altered source–sink ratio treatments during grain filling (Andrade & Ferreiro, 1996; Sala et al., 2007).

The pronounced decrease in KGR recorded during Y3 (Figure 6) can be attributed to the reduction in the assimilate availability per kernel during the critical period (i.e., PGR_{CP} kernel⁻¹; Gambín et al., 2006, 2008). The considerable reduction in the PGR_{CP} kernel⁻¹ in Y3 can be attributed to the large decrease in the PGR_{CP} that was not accompanied by a large reduction in KNP (Figures 3a and 4). The modest response of KNP to the PGR_{CP} was not surprising, since despite the latter being severely reduced, it remained above the PGR_{CP} threshold (~150 mg plant⁻¹ °C d⁻¹), beyond which no further increase in KNP is expected (Gambín et al., 2006). By contrast, such decline in PGR_{CP} kernel⁻¹ is likely to produce a decrease in individual kernel sink strength of the type recorded under reduced irradiance and linked to the decrease in the number of endosperm cells (Capitanio et al., 1983; Reddy & Daynard, 1983), with the concomitant negative effect on potential KW through a decrease in KGR (Gambín et al., 2006). This negative effect on potential KW should be reflected in a reduced KMWC as well as KMV, which are defined early in grain filling (Borrás et al., 2003; Borrás & Westgate, 2006). However, mentioned attributes were slightly constrained in Y3 (Figure 6), despite having been closely related to the estimated KW (Figure 5). This involves

the parallel but not totally linked early processes of endosperm cell division and rapid increase in kernel water content with the subsequent KGR.

4.2 | Responses of dent \times flint and flint \times flint genotypes to the changes in the grain-filling environment

The D \times F hybrids had an increased response to the changes in the explored environment for most traits (Table 3), in agreement with previous research (Tamagno et al., 2015). Despite their enhanced sensitivity to the explored growth conditions, these hybrids were consistently superior for grain yield, kernel number, and plant growth rate across all evaluated years (Table 3). This reflects the presence of strong genetic differences between both genotypic groups, which seemed to remain little affected by natural changes in environmental conditions.

Both D \times F and F \times F genotypes had a similar source–sink relationship during the critical period, since enhanced PGR_{CP} of D \times F was accompanied by an increased KNP (Figure 3a). This suggests that differences between genotypic groups in the KWm would not be related to differences in potential KW. By contrast, D \times F hybrids exhibited a reduced source–sink ratio during the effective grain filling (Table 2). In addition, a strong response of the KWm to the PG_{EGFP} kernel⁻¹ was observed for these hybrids (Figure 3c). The constrained PG_{EGFP} kernel⁻¹ observed for D \times F was mostly driven by an enhanced KNP (sink size) rather than by a reduced plant growth during grain filling, and this higher sink size would be the main cause of the increased sensitivity of D \times F KW to the changes in the assimilate supply for growing kernels (Figure 4). The opposite was observed for F \times F genotypes, because they set an increased source–sink relationship during the effective grain filling. Accordingly, a reduced KW response of F \times F to changes in environmental conditions during active grain filling was detected, with a condition of excess in the source of assimilates to fulfill kernels growth in a large proportion of F \times F hybrids by year combinations (Figure 3c), as reported by Cirilo et al. (2011) for commercial flint genotypes. Current results are supported by findings of Echarte et al. (2006), who called attention on the lower KW stability of modern semident Argentine hybrids respect to the old flint types in response to source reductions along grain filling, such as those experienced by delayed sowings (Bonelli et al., 2016) that today represent ~50% of the area cropped to maize in Argentina (Gago et al., 2018).

Despite the similar PGR_{CP} kernel⁻¹, and consequently the similar potential KW of both groups of genotypes, the F \times F hybrids exhibited on average reduced KWe, KGR, KMWC, and KMV (mostly under the most favorable environment of Y4), all grain-filling traits that strongly depend on poten-

tial kernel size. Evidently, genotypic groups differed in their capacity to use available assimilates per kernel during the LP. This assertion is supported on the fact that differences in seed composition (protein, oil, and starch proportion) implied that grains involving a larger proportion of high cost components in terms of energy (i.e., protein and oil), such as those corresponding to flints, produced a more stable KW (Tamagno et al., 2016). This response was evident for F \times F in Y4, where increases in assimilate supply per grain were not reflected in increments of KW.

5 | CONCLUSIONS

Current research contributed to understand germplasm differences in KW and its physiological determinants in response to changes in the photothermal environment explored during grain filling across a wide range of naturally variable growing conditions. Differences in the PTQs across seasons were mainly detected during active grain filling (PTQ_{EGFP}) and were predominantly linked to reduce incident solar radiation levels recorded in Y3. For this year, a marked disruption was observed between PTQs computed for each grain-filling phase, with environmental conditions during the effective grain filling that did not allow the realization of the potential established during the LP. Such condition may occur in 21% of the years for early sown maize in the region under study. Supra-optimum temperatures during the LP of Y3 had a negative effect on the potential sink determination, which was caused by a reduction in the PGR_{CP} that did not affect kernel set but promoted a decrease in the source–sink relationship, and consequently on KGR. Hybrids D \times F had increased grain yield, kernel number, and plant growth rate throughout evaluated years, but they were also much more sensitive than F \times F to stressful conditions during the effective grain filling. The narrowed source–sink ratio experienced by D \times F types during grain filling was mainly driven by their enhanced KNP respect to F \times F. This difference between genotypic groups would explain their contrasting sensitivity (D \times F > F \times F) to changes in the explored photothermal environment.

ACKNOWLEDGMENTS


We wish to thank L.B. Blanco, F. Curín, L.A. Galizia, M. Parco, M. Riveira Rubin, and A.V. Seco for their help with fieldwork. We also thank Dr. L. Borrás for his critical review of the manuscript. This research was financed by the National Agency for Science Promotion of Argentina (PICTs 1454 and 2671), the University of Buenos Aires (UBACYTs 00493), and the National Institute of Agricultural Technology (PNCYO-1127042).

CONFLICT OF INTEREST

The authors declare no conflict of interest.

ORCID

Ignacio R. Hisse  <https://orcid.org/0000-0002-5167-9557>

Karina E. D'Andrea  <https://orcid.org/0000-0003-4693-504X>

María E. Otegui  <https://orcid.org/0000-0001-9670-0316>

REFERENCES

- Abbate, P. E., Dardanelli, J. L., Cantarero, M. G., Maturano, M., Melchiori, R. J. M., & Suero, E. E. (2004). Climatic and water availability effects on water-use efficiency in wheat. *Crop Science*, *44*, 474–483. <https://doi.org/10.2135/cropsci2004.4740>
- Abdala, L., Gambín, B., & Borrás, L. (2018). Sowing date and maize grain quality for dry milling. *European Journal of Agronomy*, *92*, 1–8. <https://doi.org/10.1016/j.eja.2017.09.013>
- Andrade, F. H., & Ferreiro, M. A. (1996). Reproductive growth of maize, sunflower and soybean at different source levels during grain filling. *Field Crops Research*, *48*, 155–165. [https://doi.org/10.1016/S0378-4290\(96\)01017-9](https://doi.org/10.1016/S0378-4290(96)01017-9)
- Bonelli, L. E., Monzón, J. P., Cerrudo, A., Rizalli, R. H., & Andrade, F. H. (2016). Maize grain yield components and source-sink relationships as affected by the delay in sowing date. *Field Crops Research*, *198*, 215–225. <https://doi.org/10.1016/j.fcr.2016.09.003>
- Borrás, L., & Otegui, M. E. (2001). Maize kernel weight response to post flowering source-sink ratio. *Crop Science*, *41*, 1816–1822. <https://doi.org/10.2135/cropsci2001.1816>
- Borrás, L., Slafer, G. A., & Otegui, M. E. (2004). Seed dry weight response to source-sink manipulations in wheat, maize and soybean: A quantitative reappraisal. *Field Crops Research*, *86*, 131–146. <https://doi.org/10.1016/j.fcr.2003.08.002>
- Borrás, L., Westgate, M. E., & Otegui, M. E. (2003). Control of kernel weight and kernel water relations by post-flowering source-sink ratio in maize. *Annals of Botany*, *91*, 857–867. <https://doi.org/10.1093/aob/mcg090>
- Borrás, L., & Westgate, M. E. (2006). Predicting maize kernel sink capacity early in development. *Field Crops Research*, *95*, 223–233. <https://doi.org/10.1016/j.fcr.2005.03.001>
- Capitanio, R., Gentinetta, E., & Motto, M. (1983). Grain weight and its components in maize inbred lines. *Maydica*, *28*, 365–379.
- Cicchino, M., Rattalino Edreira, J. I., Uribealrea, M., & Otegui, M. E. (2010). Heat stress in field-grown maize: Response of physiological determinants of grain yield. *Crop Science*, *50*, 1438–1448. <https://doi.org/10.2135/cropsci2009.10.0574>
- Cirilo, A. G., Actis, M., Andrade, F. H., & Valentinuz, O. R. (2011). Crop management affects dry-milling quality of flint maize kernels. *Field Crops Research*, *122*, 140–150. <https://doi.org/10.1016/j.fcr.2011.03.007>
- Cirilo, A. G., & Andrade, F. H. (1996). Sowing date and kernel weight in maize. *Crop Science*, *36*, 325–331. <https://doi.org/10.2135/cropsci1996.011183X003600020019x>
- Cooper, M., Woodruff, D. R., Eisemann, R. L., Brennan, P. S., & DeLacy, I. H. (1995). A selection strategy to accommodate genotype by environment interaction for grain yield of wheat: Managed-environments for selection among genotypes. *Theoretical and Applied Genetics*, *90*, 492–502. <https://doi.org/10.1007/bf00221995>
- D'Andrea, K. E., Otegui, M. E., Cirilo, A. G., & Eyhéabide, G. H. (2006). Genotypic variability in morphological and physiological traits among maize inbred lines I. Response to nitrogen availability. *Crop Science*, *46*, 1266–1276. <https://doi.org/10.2135/cropsci2005.07-0195>
- de la Vega, A., & Chapman, S. C. (2001). Genotype by environment interaction and indirect selection for yield in sunflower: II. Three-mode principal component analysis of oil and biomass yield across environments in Argentina. *Field Crops Research*, *72*, 39–50. [https://doi.org/10.1016/S0378-4290\(01\)00163-0](https://doi.org/10.1016/S0378-4290(01)00163-0)
- Di Matteo, J. A., Ferreyra, J. M., Cerrudo, A. A., Echarte, L., & Andrade, F. H. (2016). Yield potential and yield stability of Argentine maize hybrids over 45 years of breeding. *Field Crops Research*, *197*, 107–116. <https://doi.org/10.1016/j.fcr.2016.07.023>
- Echarte, L., Andrade, F. H., Sadras, V. O., & Abbate, P. (2006). Kernel weight and its response to source manipulations during grain filling in Argentinean maize hybrids released in different decades. *Field Crops Research*, *96*, 307–312. <https://doi.org/10.1016/j.fcr.2005.07.013>
- Fischer, R. A. (1985). Number of kernels in wheat crops and the influence of solar radiation and temperature. *The Journal of Agricultural Science*, *105*, 447–461. <https://doi.org/10.1017/S0021859600056495>
- Gago, A., Gianatiempo, J. P., & López, M. (2018). *La cadena del maíz en la Argentina: Evolución del cultivo durante las últimas campañas*. Bolsa de Cereales. Retrieved from <https://www.bolsadecereales.com/imagenes/retaa/2018-12/161-lacadenademaizena-rgentinaretaapaseee09.11.2018.pdf>
- Gallo, K. P., & Daughtry, C. S. T. (1986). Techniques for measuring intercepted and absorbed photosynthetically active radiation in corn canopies. *Agronomy Journal*, *78*, 752–756. <https://doi.org/10.2134/agronj1986.00021962007800040039x>
- Gambín, B. L., Borrás, L., & Otegui, M. E. (2006). Source-sink relations and kernel weight differences in maize temperate hybrids. *Field Crops Research*, *95*, 316–326. <https://doi.org/10.1016/j.fcr.2005.04.002>
- Gambín, B. L., Borrás, L., & Otegui, M. E. (2007). Kernel water relations and duration of grain filling in maize temperate hybrids. *Field Crops Research*, *101*, 1–9. <https://doi.org/10.1016/j.fcr.2006.09.001>
- Gambín, B. L., Borrás, L., & Otegui, M. E. (2008). Kernel weight dependence upon plant growth at different grain-filling stages in maize and sorghum. *Australian Journal of Agricultural Research*, *59*, 280–290. <https://doi.org/10.1071/AR07275>
- Hisse, I. R., D'Andrea, K. E., & Otegui, M. E. (2019). Source-sink relations and kernel weight in maize inbred lines and hybrids: Responses to contrasting nitrogen supply levels. *Field Crops Research*, *230*, 151–159. <https://doi.org/10.1016/j.fcr.2018.10.011>
- Jones, R. J., & Simmons, S. R. (1983). Effect of altered source-sink ratio on growth of maize kernels. *Crop Science*, *23*, 129–134. <https://doi.org/10.2135/cropsci1983.0011183X002300010038x>
- Kiniry, J. R., & Otegui, M. E. (2000). Processes affecting maize grain yield potential in temperate conditions. In M. E. Otegui & G. A. Slafer (Eds.), *Physiological bases for maize improvement* (pp. 31–46). Food Products Press, The Haworth Press.
- Maddonni, G. A. (2012). Analysis of the climatic constraints to maize production in the current agricultural region of Argentina—a probabilistic approach. *Theoretical and Applied Climatology*, *107*, 325–345. <https://doi.org/10.1007/s00704-011-0478-9>
- Magrin, G. O., Marengo, J. A., Boulanger, J. P., Buckeridge, M. S., Castellanos, E., Poveda, G., Scarano, F. R., & Vicuña, S. (2014). Part B: Regional aspects. Contribution of working group II to the fifth assessment report of the intergovernmental panel on climate change. In V. R. Barros & C. B. Field (Eds.), *Climate change 2014: Impacts, adaptation, and vulnerability* (pp. 1499–1566). Cambridge University Press.

- Melchiori, R. J. M., & Caviglia, O. P. (2008). Maize kernel growth and kernel water relations as affected by nitrogen supply. *Field Crops Research*, *108*, 198–205. <https://doi.org/10.1016/j.fcr.2008.05.003>
- Messina, C. D., Hammer, G. L., McLean, G., Cooper, M., van Oosterom, E. J., Tardieu, F., Chapman, S. C., Doherty, A., & Gho, C. (2019). On the dynamic determinants of reproductive failure under drought in maize. *Silico Plants*, *1*, 1–14. <https://doi.org/10.1093/insilicoplants/diz003>
- Muchow, R. C. (1990). Effect of high temperature on grain-growth in field-grown maize. *Field Crops Research*, *23*, 145–158. [https://doi.org/10.1016/0378-4290\(90\)90109-O](https://doi.org/10.1016/0378-4290(90)90109-O)
- NeSmith, D. S., & Ritchie, J. T. (1992). Maize (*Zea mays*, L.) response to a severe soil water-deficit during grain-filling. *Field Crops Research*, *29*, 23–25. [https://doi.org/10.1016/0378-4290\(92\)90073-I](https://doi.org/10.1016/0378-4290(92)90073-I)
- Ouattar, S., Jones, R. J., & Crookston, R. K. (1987). Effect of water deficit during grain filling on the pattern of maize kernel growth and development. *Crop Science*, *27*, 726–730. <https://doi.org/10.2135/cropsci1987.0011183X002700040025x>
- Ouattar, S., Jones, J. R., Crookston, R. K., & Kajeiou, M. (1987). Effect of drought on water relations of developing maize kernels. *Crop Science*, *27*, 730–735. <https://doi.org/10.2135/cropsci1987.0011183X002700040026x>
- R Core Team. (2018). *R: A language and environment for statistical computing*. R Foundation for Statistical Computing.
- Radushev, D. (2007). *Graph Pad Prism version 5.0*. Graph Pad Software.
- Rattalino Edreira, J. I., Mayer, J. I., & Otegui, M. E. (2014). Heat stress in temperate and tropical maize hybrids: Kernel growth, water relations and assimilate availability for grain filling. *Field Crops Research*, *166*, 162–172. <https://doi.org/10.1016/j.fcr.2014.06.018>
- Rattalino Edreira, J. I., & Otegui, M. E. (2012). Heat stress in temperate and tropical maize hybrids: Differences in crop growth, biomass partitioning and reserves use. *Field Crops Research*, *130*, 87–98. <https://doi.org/10.1016/j.fcr.2012.02.009>
- Reddy, V. H., & Daynard, T. B. (1983). Endosperm characteristics associated with rate of grain filling and kernel size in corn. *Maydica*, *28*, 339–355.
- Ritchie, J. T., & NeSmith, D. S. (1991). Temperature and crop development. In J. Hanks & J. T. Ritchie (Eds.), *Modelling plant and soil systems, agronomy series 31* (pp. 5–29). ASA, CSSA, and SSSA.
- Ritchie, S. W., Hanway, J. J., & Benson, G. O. (1992). *How a plant crop develops*. Iowa State University of Science and Technology.
- Rotundo, J. L., Tang, T., & Messina, C. D. (2019). Response of maize photosynthesis to high temperature: Implications for modeling the impact of global warming. *Plant Physiology and Biochemistry*, *141*, 202–205. <https://doi.org/10.1016/j.plaphy.2019.05.035>
- Sala, R. G., Westgate, M. E., & Andrade, F. H. (2007). Source/sink ratio and the relationship between maximum water content, maximum volume, and final dry weight of maize kernels. *Field Crops Research*, *101*, 19–25. <https://doi.org/10.1016/j.fcr.2006.09.004>
- Shekoofa, A., Sinclair, T. R., Messina, C. D., & Cooper, M. (2016). Variation among maize hybrids in response to high vapor pressure deficit at high temperatures. *Crop Science*, *56*, 392–396. <https://doi.org/10.2135/cropsci2015.02.0134>
- Stockle, C. O., & Kiniry, J. R. (1990). Variability in crop radiation-use efficiency associated with vapor-pressure deficit. *Field Crops Research*, *25*, 171–181. [https://doi.org/10.1016/0378-4290\(90\)90001-R](https://doi.org/10.1016/0378-4290(90)90001-R)
- Tamagno, S., Greco, I. A., Almeida, H., & Borrás, L. (2015). Physiological differences in yield related traits between flint and dent Argentinean commercial maize genotypes. *European Journal of Agronomy*, *68*, 50–56. <https://doi.org/10.1016/j.eja.2015.04.001>
- Tamagno, S., Greco, I. A., Almeida, H., Di Paola, J. C., Martí Ribes, F., & Borrás, L. (2016). Crop management options for maximizing maize kernel hardness. *Agronomy Journal*, *108*, 1–10. <https://doi.org/10.2134/agronj2015.0590>
- Tollenaar, M. (1983). Potential vegetative productivity in Canada. *Canadian Journal of Plant Science*, *63*, 1–10.
- Tsimba, R., Edmeades, G. O., Millner, J. P., & Kemp, P. D. (2013). The effect of planting date on maize grain yields and yield components. *Field Crops Research*, *150*, 135–144. <https://doi.org/10.1016/j.fcr.2013.05.021>
- Vega, C. R. C., Sadras, V. O., Andrade, F. H., & Uhart, S. A. (2000). Reproductive allometry in soybean, maize and sunflower. *Annals of Botany*, *85*, 461–468. <https://doi.org/10.1006/anbo.1999.1084>
- Wahid, A., Gelani, S., Ashraf, M., & Foolad, M. R. (2007). Heat tolerance in plants: An overview. *Environmental and Experimental Botany*, *61*, 199–223. <https://doi.org/10.1016/j.envexpbot.2007.05.011>
- Westgate, M. E. (1994). Water status and development of the maize endosperm and embryo during drought. *Crop Science*, *34*, 76–83. <https://doi.org/10.2135/cropsci1994.0011183X003400010014x>

SUPPORTING INFORMATION

Additional supporting information may be found online in the Supporting Information section at the end of the article.

How to cite this article: Hisse IR, D'Andrea KE, Otegui ME. Kernel weight responses to the photothermal environment in maize dent × flint and flint × flint hybrids. *Crop Science*. 2021;1–16. <https://doi.org/10.1002/csc2.20481>